CHEMISTRY OF MATERIALS

Article

pubs.acs.org/cm

Surfactant-Templated Synthesis of Ordered Silicas with Closed Cylindrical Mesopores

Manik Mandal[†,§] and Michal Kruk*[,†,‡]

[†]Center for Engineered Polymeric Materials, Department of Chemistry, College of Staten Island, City University of New York, 2800 Victory Boulevard, Staten Island, New York 10314, United States

[‡]Graduate Center, City University of New York, 365 Fifth Avenue, New York, New York 10016, United States

Supporting Information

ABSTRACT: Ordered mesoporous silicas with 2-dimensional hexagonal arrays of closed cylindrical pores were synthesized via templating with block copolymer surfactant followed by calcination at appropriately high temperatures. Precursors to closed-pore silicas, including SBA-15 silicas and organosilicas, were selected based on the existence of narrow passages to the mesopores. The increase in calcination temperature to 800−950 °C led to a dramatic decrease in nitrogen uptake by the materials, indicating the loss of accessible mesopores, whereas small-angle X-ray scattering (SAXS) indicated no major structural changes other than the framework shrinkage. Since SAXS patterns for ordered mesoporous materials are related to periodic arrays of mesopores, the existence of closed mesopores was evident, as additionally confirmed by TEM. The formation of closed-pore silicas was demonstrated for ultralarge-pore SBA-15 and large-pore phenylene-bridged periodic mesoporous organosilicas. The increase in the amount of tetraethyl orthosilicate in standard SBA-15 synthesis also allowed us to observe the thermally induced pore closing. It is hypothesized that the presence of porous plugs in the cylindrical mesopores and/or caps at their ends was responsible for the propensity to the pore closing at sufficiently high temperatures. The observed behavior is likely to be relevant to a variety of silicas and organosilicas with cylindrical mesopores.

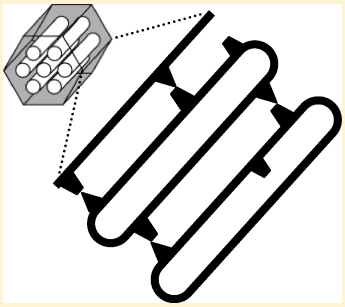

KEYWORDS: *closed-pore material, SBA-15, periodic mesoporous organosilica, 2-D hexagonal silica, micelle-templated synthesis*

INTRODUCTION

The micelle-templating approach[1,2] has revolutionized the synthesis of well-defined mesoporous materials.[3,4] This appoach was first demonstrated on ordered mesoporous silicas[1,2,5,6] and then extended on a variety of other framework compositions.[7−11] More recently, the single-micelle templating emerged as a convenient pathway for the synthesis of hollow spherical nanoparticles and nanotubes.[12−16] A remarkable feature of the micelle-templating approach is that it can lead to open-pore materials, as expected from the fact that the surfactant template needs to be removed from the mesopores,[1,5] as well as to closed-pore materials.[17−25] However, the direct surfactant-templating pathway to closed-pore structures has been demonstrated only for materials with spherical mesopores.[17−25] Herein, it is shown that closed-pore materials can also be generated for a cylindrical pore geometry.

At first, materials with cylindrical mesopores templated by cylindrical micelles do not appear to be good candidates for closed-pore materials, unless the modification of their external surface is performed.[26] However, it has been reported that the synthesis of well-known open-pore SBA-15 silica with cylindrical mesopores templated by Pluronic P123 ($EO_{20}PO_{70}EO_{20}$) block copolymer micelles using tetraethylorthosilicate (TEOS) as a framework precursor can be adjusted through the increase in the ratio of TEOS to the surfactant to render silicas with 2-dimensional (2-D) hexagonal ordering and with constrictions (porous "plugs"), hypothesized to be in the mesopores.[27,28] The formation of the porous plugs was attributed to the solubilization of excess TEOS in the hydrophobic cores of the Pluronic P123 micelles, and its subsequent condensation into deposits in the cylindrical mesoporous voids of SBA-15 silica framework.[28] The mesopores (diameter about 6 nm) of one of the plugged SBA-15 silicas were made inaccessible through the surface modification with organosilyl groups of sufficiently large size, revealing that the cylindrical mesopores were accessible through entrances about 3 nm in diameter.[29] The formation of the "plugged" mesopores was found to be quite common for Pluronic-templated 2-D hexagonal materials with cylindrical mesopores, including ultralarge-pore SBA-15 silica synthesized at low initial temperature (10−17 °C) without hydrothermal treatment[30,31] and large-pore periodic mesoporous organosilicas (PMOs).[32] Another finding that points out to the feasibility of converting the well-known open-pore surfactant-templated materials with cylindrical mesopores to closed-pore materials was the observation of hemispherical caps on the pore ends in Pluronic-templated organosilica materials with cylindrical mesopores.[32]

Herein, the successful synthesis of ordered mesoporous silicas with closed cylindrical mesopores through thermally

Received: August 29, 2011
Revised: November 19, 2011
Published: November 28, 2011

induced pore closing is reported, and structural features of materials that enable the formation of the closed cylindrical mesopores are discussed.

MATERIALS AND METHODS

Synthesis of SBA-15 Silica. Mesoporous SBA-15 silica was synthesized using Pluronic P123 ($EO_{20}PO_{70}EO_{20}$) as a structure directing agent and tetraethylorthosilicate (TEOS) as a silica source, according to a literature procedure,[5,33] but with a doubled amount of TEOS[28,29] and without the hydrothermal treatment. Specifically, 2.0 g of Pluronic P123 was dissolved in 14 g of water and 61 g of 1.97 M HCl solution. Then, 8.60 g of TEOS was added, and the resulting mixture was stirred at 35 °C for one day. Then the as-synthesized material was filtered, washed with water, and dried in a vacuum oven at temperature set at about 60 °C. Finally, the sample was calcined under air at 550 °C for 5 h (heating ramp 2 °C min^{-1}) or at a higher temperature.

Synthesis of Ultralarge-Pore SBA-15 Silica. Ultralarge-pore SBA-15 (ULP-SBA-15) silica was synthesized using Pluronic P123 as a structure-directing agent and TEOS as silica source, following our earlier work.[30] 2.4 g of P123 and 0.027 g of NH_4F were dissolved in 84.0 mL of 1.30 M aqueous solution at room temperature under mechanical stirring. Subsequently, the solution was placed in a water bath (nominal temperature accuracy of 0.01 °C) set at 13 °C, and after 1 h, a mixture of 5.5 mL of TEOS and 2.4 mL (2.0 g) of 1,3,5-triisopropylbenzene (TIPB) was added under mechanical stirring. The solution was stirred for 1 d at 13 °C in an open container. Then the product was isolated by filtering, washing with water, and drying at about 60 °C in a vacuum oven. Finally the sample was calcined under air at 550 °C for 5 h (heating ramp 2 °C min^{-1}) or at a higher temperature.

Synthesis of Phenylene-Bridged PMO with a 2-Dimensional Hexagonal Structure. Periodic mesoporous organosilica with phenylene bridging groups and a 2-dimensional hexagonal structure was synthesized as reported elsewhere.[32] 0.60 g of Pluronic P123 was dissolved in 21 mL of 1.30 M HCl solution under mechanical stirring at 18 °C. Then, premixed 1.95 mL of 1,4-bis(triethoxysilyl)benzene and 0.6 mL TIPB were added. The solution was stirred at 18 °C for 1 d and subsequently hydrothermally treated in a polypropylene bottle at 100 °C for 2 d. As-synthesized material was filtered, washed, dried, and calcined under nitrogen at 300 °C for 5 h (heating ramp 2 °C min^{-1}) or under air at higher temperatures.

Measurements. The small-angle X-ray scattering patterns were measured on Bruker Nanostar U instrument equipped with Cu K_α radiation source (rotating anode operated at 50 kV, 24 mA) and Vantec-2000 2-dimensional detector. Samples were placed in the hole of an aluminum sample holder and secured with a Kapton tape. Nitrogen adsorption isotherms were acquired on a Micromeritics ASAP 2020 volumetric adsorption analyzer at −196 °C. The samples were outgassed at 140 °C in the port of the adsorption analyzer before the analysis. Transmission electron microscopy (TEM) images were collected on FEI Tecnai G2 Spirit microscope operated at an accelerating voltage of 120 kV. The samples were sonicated in ethanol and subsequently drop-casted on a carbon-coated copper grid. The solvent was allowed to evaporate under air before imaging.

Calculations. The BET specific surface area (S_{BET}) was determined from nitrogen adsorption isotherm in the relative pressure range from 0.04 to 0.20. Total pore volume (V_t) was determined from the amount adsorbed at a relative pressure of 0.99. Pore size distributions (PSDs) were determined from adsorption branches of the isotherms using the Barrett–Joyner–Halenda (BJH) method with the KJS correction.[34]

RESULTS AND DISCUSSION

In the attempt to synthesize a micelle-templated material with closed cylindrical mesopores, ultralarge-pore SBA-15 silica was synthesized at 13.0 °C using Pluronic P123 as a surfactant, 1,3,5-triisopropylbenzene (TIPB) as a swelling agent, and tetraethyl orthosilicate (TEOS) as a silica source using a procedure reported earlier,[30] but without the hydrothermal treatment. The as-synthesized material exhibited 2-D hexagonal structure with (100) interplanar spacing, d_{100}, of 24.9 nm, which was significantly reduced (to 20.1 nm, which is a 19% decrease; see Supporting Information Table S1) as a result of calcination at 550 °C (see small-angle X-ray scattering, SAXS, patterns in Figure 1). Large shrinkage is typical for ordered

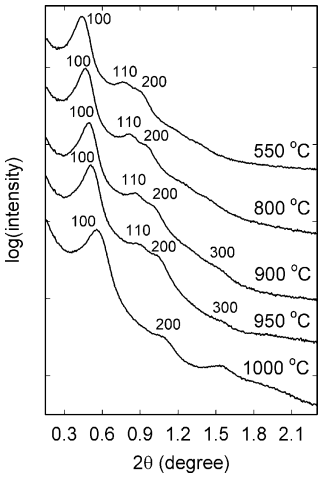

Figure 1. Small-angle X-ray scattering patterns of ultralarge-pore SBA-15 synthesized at low temperature without hydrothermal treatment and calcined at different temperatures.

mesoporous silicas prepared at low temperature only.[31] As expected from earlier reports of SBA-15 synthesized at low temperatures (15–17 °C) with hexane or TIPB as swelling agents,[30,31] the considered SBA-15 silica exhibited a broad adsorption–desorption hysteresis loop with capillary evaporation at the lower limit of adsorption–desorption hysteresis (relative pressure about 0.50; see Figure 2), indicating that the

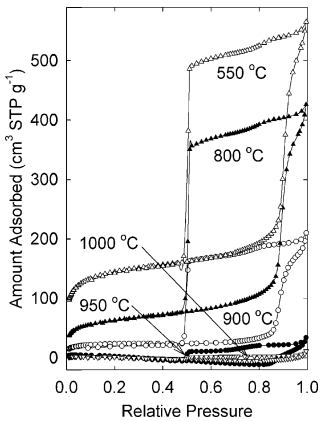

Figure 2. Nitrogen adsorption isotherms for ULP-SBA-15 synthesized at low temperature without hydrothermal treatment and calcined at different temperatures.

entrances to its mesopores (or constrictions in them) were of diameter below 5 nm.[35] The size of these passages was much smaller than the BJH (nominal) diameter of 21.0 nm (which corresponds to an actual diameter of about 17 nm)[30] for cylindrical mesopores in the material.

dx.doi.org/10.1021/cm202577g | Chem. Mater. 2012, 24, 149–154

When the calcination temperature was increased, the interplanar spacing decreased, but the resolution of SAXS patterns remained the same up to 950 °C (Figure 1 and Supporting Information Table S1; d_{100} was reduced by 31% to 17.3 nm at 950 °C), while the pattern was somewhat less resolved after calcination at 1000 °C. Despite the similarity of SAXS patterns, the materials calcined at different temperatures had dramatically different adsorption capacities. The sample calcined at 550 °C had a total pore volume, V_t, of 0.85 cm^3/g (see Supporting Information Table S1). While a decrease in the adsorption capacity was moderate when the calcination temperature increased from 550 to 800 °C, a further increase to 900 °C led to a 2-fold decrease in the total pore volume, while the increase to 950 °C reduced the adsorption capacity to about one-tenth of that after calcination at 550 °C. The calcination at 1000 °C reduced the uptake of N_2 even further. The adsorption isotherms for the samples calcined at 950–1000 °C were somewhat distorted (showing a decrease in adsorbed amount as the pressure increased), because the adsorption capacity of these samples was too low to obtain high-quality data using 30–60 mg sample, which was sufficient for higher-adsorption-capacity materials obtained after calcination at 900 °C or lower. The dramatic decrease in the adsorption capacity observed starting from 900 °C cannot be attributed to the decrease in the unit-cell size only, because this decrease was moderate (see Supporting Information Table S1). The major decrease in the adsorption capacity was not accompanied by the loss of SAXS pattern resolution and intensity (except for calcination at 1000 °C), so the observed behavior points to a transition from accessible mesopores to inaccessible ones as the calcination temperature increased to 900 °C or higher. The examination of pore size distributions (Figure 3) indicates that the calcination-induced pore size

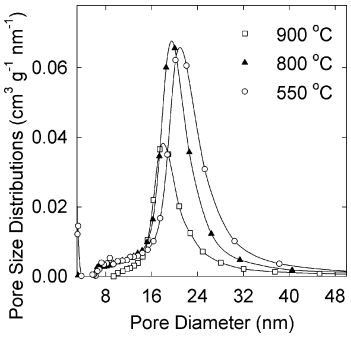

Figure 3. Pore size distributions of ULP-SBA-15 synthesized at low temperature without hydrothermal treatment and calcined at different temperatures.

decrease was quite limited (see also Supporting Information Table S1). The retention of the ordered mesopore structure at 950 °C was additionally confirmed by transmission electron microscopy (TEM) (see Figure 4 showing a thin region of the sample and Supporting Information Figures S1–S4). The observed behavior of SBA-15 silica with cylindrical mesopores prepared at low temperature was similar to that observed earlier for ordered mesoporous silicas and organosilicas with spherical mesopores[21–24,36] and was markedly different from that of a typical SBA-15 silica,[5,33,37,38] for which there was no evidence of thermally induced pore closing despite a significant structural shrinkage during calcination at around 1000 °C.[38–41]

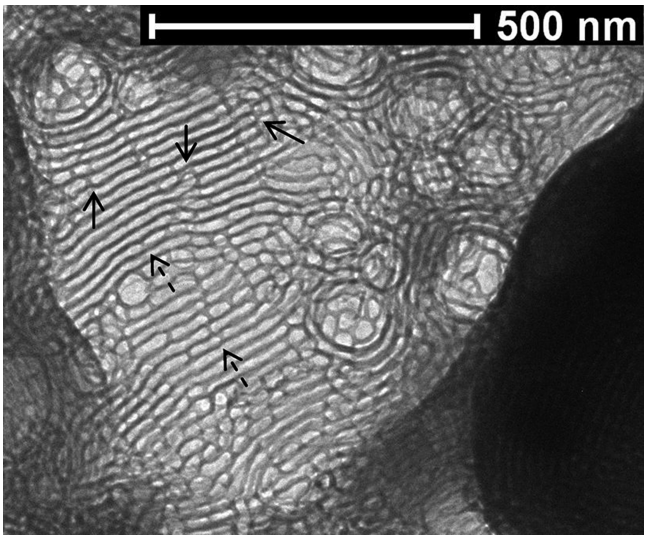

Figure 4. Transmission electron microscopy image of ULP-SBA-15 calcined at 950 °C. Solid-line arrows point to mesopores that appear to have hemispherical ends, while dashed-line arrows point to apparent plugs in the mesopores.

As was discussed in our earlier reports,[30,31,42] large-pore SBA-15 synthesized at subambient temperatures in the presence of a swelling agent (hexane or TIPB) without hydrothermal treatment or with hydrothermal treatment at moderate temperature or for short periods of time exhibited surprisingly narrow entrances to the mesopores, which were attributed to constrictions (perhaps porous plugs) in the mesopores.[30,31,42] Appropriately long hydrothermal treatment times or/and high temperatures were needed to remove the constrictions.[30,31,42] A study of related organosilicas pointed to a possibility of the presence of caps at the ends of cylindrical mesopores.[32] TEM imaging of our SBA-15 material provided some evidence of the presence of plugs in the mesopores and hemispherical caps at pore ends (Figure 4 and Supporting Information Figures S1–S4). The results presented herein suggest that at sufficiently high calcination temperature, the constrictions and/or caps consolidate and close the access to the mesopores (see Scheme 1).

Scheme 1. Proposed Mechanism of the Thermally-Induced Closing of Cylindrical Mesopores with Porous Plugs and/or Caps As a Process Involving the Formation of Impermeable Plugs Inside the Mesopores and/or Closed Caps at the Mesopore Ends

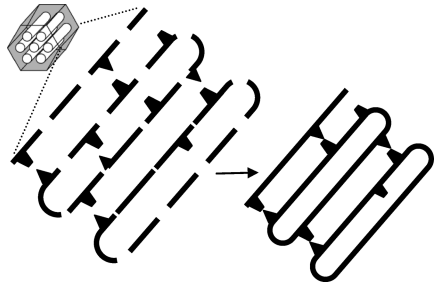

This is in contrast to the case of standard synthesis of SBA-15, for which there was no evidence that the mesopores can be closed, even though the structure shrinks dramatically at 970–1000 °C.[39,40] However, it is known that when the relative amount of TEOS to the block copolymer surfactant is increased

dx.doi.org/10.1021/cm202577g | Chem. Mater. 2012, 24, 149–154

in otherwise standard SBA-15 synthesis, the constrictions develop in the mesopores.[28,29] Guided by this prior work, standard SBA-15 synthesis at 35 °C was modified by doubling the amount of TEOS and isolating the material without subjecting it to a hydrothermal treatment typically involved in the SBA-15 synthesis. While the obtained sample had 2-D hexagonal ordering, as seen from SAXS (Supporting Information Figure S5), it had a small pore size and low adsorption capacity after calcination at 550 °C. It should be noted that a regular synthesis of SBA-15 at 35 °C without the hydrothermal treatment also affords a sample with quite small pore diameter (~5 nm) and low mesopore volume.[5,33] The increase in the calcination temperature to 800 °C led to a major decrease in the specific surface area (see Supporting Information Table S1), which can be attributed to the elimination of the framework microporosity, the latter having been observed for regular SBA-15 at 880−1000 °C,[33,40] and finally our material no longer adsorbed nitrogen after calcination at 950 °C (Supporting Information Figure S5). Still, a well-resolved SAXS pattern was observed for the samples calcined at the latter temperature, which resembled the patterns recorded for the same sample calcined at lower temperatures of 550−900 °C, showing that in this case, the periodic mesoporous structure of SBA-15 was retained at 950 °C despite the fact that the mesopores were no longer accessible to nitrogen molecules.

To extend the scope of the method, the opportunities in the pore closing were explored for periodic mesoporous organosilicas (PMOs) with bridging organic groups in silica-type frameworks.[43−45] 2-D hexagonal large-pore phenylene-bridged PMOs[32] were selected, because of high thermal stability of this kind of bridging groups,[46] and because of the presence of narrow openings to the large mesopores of such PMOs.[32] While in our hands, it has not yet been possible to achieve the mesopore closing without the degradation of the organic bridging groups, the PMO was successfully converted to a closed-pore silica. As seen from nitrogen adsorption, the large mesopores were nearly inaccessible after calcination at 800 and 850 °C (see Supporting Information Figure S6), whereas well-defined SAXS patterns were observed. TEM images (Figure 5 and Supporting Information Figure S7) provided some evidence of the caps on the pore ends. It should be noted that the residual accessible mesopores observed at these temperatures might have been related to ends or parts of cylindrical mesopores that did not feature caps or plugs (see Figure 5) or to onion-type impurity domains (Figure 5), which were seen for this PMO in TEM.

The unusual propensity of the cylindrical mesopores of the materials discussed above to close as a result of the thermal treatment can be attributed to the presence of narrow passages to the mesopores (as seen from broad hysteresis loops on nitrogen adsorption isotherms for the large-pore materials considered herein). The narrow passages may be constrictions (porous plugs) in the mesopore interior and/or pores in caps at the mesopore ends (see Scheme 1). Apparently, the pores in the plugs and/or caps shrink as the material is heated and eventually their size decreases below the size of nitrogen molecules that are used to probe the pore accessibility. Perhaps the connecting pores completely close (sinter) as the framework consolidates. Such a pore closing mechanism would be similar to that already proposed for the formation of surfactant-templated ordered silicas with closed spherical mesopores.[21] It should be noted that the narrow passages that can be thermally closed (or reduced in size so much that they no longer can be passed by nitrogen molecules) are not likely to be readily visible in TEM, because of their small size and disordered nature. This is because connecting pores (primarily micropores) in regular SBA-15 silicas[33,38] have not been successfully visualized by TEM, although the connections enlarged by hydrothermal treatments at high temperatures (about 130 °C or higher) assume sizes in the mesopore range and were observable by TEM.[47,48] However, such SBA-15 silicas are not expected to be amenable to the thermally induced mesopore closing.

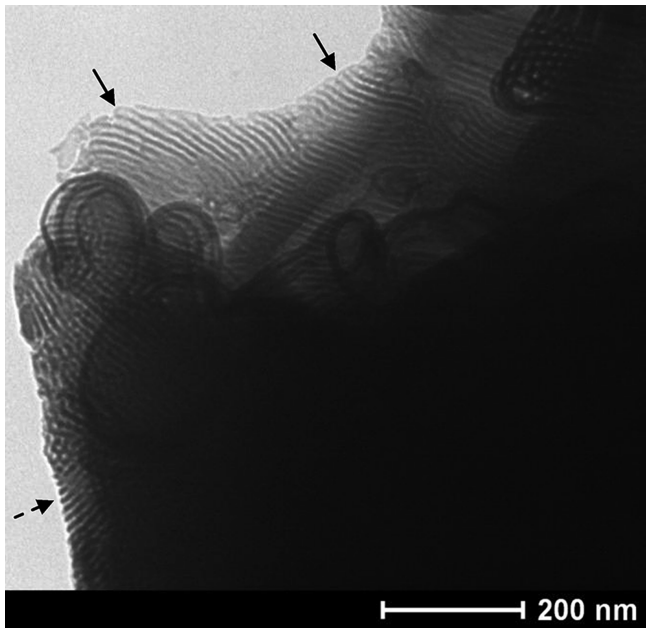

Figure 5. Transmission electron microscopy image of 2-D hexagonal silica derived from phenylene-bridged periodic mesoporous organosiloca calcined at 850 °C. Solid-line arrows point to mesopores that appear to have caps at the ends, while a dashed-line arrow points to apparently open-ended mesopores.

The porous plugs are known to develop in regular synthesis of SBA-15 as the TEOS/Pluronic ratio is increased. Their occurrence was attributed to the solubilization of excess TEOS in the hydrophobic domains of the block copolymer template.[28] Low temperature syntheses of SBA-15 silica and 2-D hexagonal PMOs also involve the formation of the plugs, although extended hydrothermal treatments can eliminate them in the case of SBA-15 and some PMOs.[30,32] Also, due to the formation of the framework in the hydrophilic domains (PEO-based) of the block copolymer micelles, the templated materials with cylindrical mesopores (e.g., SBA-15) may exhibit caps at pore ends, at least at early stages of their formation. Some evidence of caps at pore ends was seen in the synthesis of 2-D hexagonal PMOs,[32] and additional evidence was provided above in the present study. The formation of the caps can readily be explained as a result of the condensation of the framework precursor in the PEO envelope of the PEO-based surfactant micelles,[49,50] in which case, there is no reason why the framework would not form on the hemispherical ends of the micelles. However, the walls of the final periodic material form through the condensation of the framework precursor layers located within PEO envelopes of two or more adjacent micelles, whereas the caps on the ends of the micelles would not be reinforced. Therefore, the caps at the pore ends may be thinner than the walls of the honeycomb structure and may be removed during the hydrothermal treatments typically involved

in SBA-15 synthesis. On the other hand, it is possible that at early stages of SBA-15 synthesis in which the elongation of cylindrical micelles is likely to take place,[51] the micelles elongate by meeting end-to-end, while their caps at the ends either open or are retained and distort/consolidate into plugs. TEM images for our SBA-15 silica (see for instance Figure 1 and Supporting Information Figure S3) are consistent with this mechanism of the plug formation. It is expected that many other synthesis procedures may involve plug or cap formation (the latter primarily for materials templated by PEO-based surfactants, such as PEO-PPO-PEO block copolymers or oligo(ethylene oxide)-alkyl surfactants[5,37]), and thus the resulting materials may be amenable to the pore closing at sufficiently high temperatures.

Significant shrinkage of the structure was observed to be involved in the pore closing events, both for spherical[21−24,36] and cylindrical mesopores. Herein, 24−35% decrease in the interplanar spacing with respect to as-synthesized materials was seen after the calcination at temperatures that led to the pore closing. While it is uncommon in the synthesis of porous silicas or organosilicas in powder form to observe such significant shrinkage upon calcination, enormous shrinkage accompanies the surfactant removal in many micelle-templated thin films[52] and monoliths.[53] Therefore, it is likely that in some cases of silica or organosilica films or monoliths templated by PEO-based surfactants, cylindrical mesopores in some parts of the material may close in a manner similar to that reported in the present study for materials in the powder form. Therefore, our work can serve as a useful guide as for the possibility of the pore closing. In particular, it suggests that factors hindering the formation of the plugs and retention of caps at pore ends (if the caps indeed form, as expected on the basis of the discussion above) and decreasing the shrinkage, such as low framework-precursor/surfactant ratios or extensive hydrothermal treatment, can be employed if open-pore materials are sought. The opposite strategy, involving high framework-precursor/surfactant ratios and/or no (or limited) hydrothermal treatment, can be used to promote the formation of the closed mesopores through the thermally induced pore closure. The new opportunities in the engineering of the pore accessibility presented herein are expected to contribute to the ongoing effort on the design of low dielectric constant materials with closed mesopores.[19,54,55]

CONCLUSIONS

An appropriate selection of conditions in the synthesis involving PEO-containing micelle templates, such as Pluronic P123 block copolymer, affords 2-D hexagonally ordered material with cylindrical mesopores that are susceptible to the thermally induced closure. The precursors to the closed-pore silicas with cylindrical mesopores can be selected from SBA-15 silicas as well as 2-D hexagonal periodic mesoporous organosilicas (PMOs). The pore closure takes place at temperatures of 800 °C or higher. Further work will be needed to assess the feasibility of the synthesis of closed-pore PMOs with retention of the organic bridging groups. The pore closing is postulated to involve the consolidation of the constrictions (porous plugs) in the cylindrical mesopores and/or caps at the mesopore ends.

ASSOCIATED CONTENT

Supporting Information

Figures with TEM images, SAXS patterns, nitrogen adsorption isotherms and pore size distributions. Table with structural parameters derived from SAXS and nitrogen adsorption data. This material is available free of charge via the Internet at http://pubs.acs.org.

AUTHOR INFORMATION

Corresponding Author

*E-mail: Michal.Kruk@csi.cuny.edu.

Present Address

[§]Department of Chemistry, Lehigh University, Bethlehem, PA 18015.

Author Contributions

The manuscript was written through contributions of all authors. All authors have given approval to the final version of the manuscript.

ACKNOWLEDGMENTS

NSF is gratefully acknowledged for support of this research (award DMR-0907487) and for funding the acquisition of SAXS/WAXS system through award CHE-0723028. Acknowledgment is made to the Donors of the American Chemical Society Petroleum Research Fund for partial support of this research (Award PRF #49093-DNI5). The Imaging Facility at CSI is acknowledged for providing access to TEM. BASF is acknowledged for the donation of the Pluronic P123 block copolymer.

ABBREVIATIONS

2-D, two-dimensional; PEO, poly(ethylene oxide); PEO-PPO-PEO, poly(ethylene oxide)-poly(propylene oxide)-poly(ethylene oxide); PMO, periodic mesoporous silica; SAXS, small-angle X-ray scattering; TEM, transmission electron microscopy; TEOS, tetraethyl orthosilicate; TIPB, 1,3,5-triisopropylbenzene

REFERENCES

(1) Beck, J. S.; Vartuli, J. C.; Roth, W. J.; Leonowicz, M. E.; Kresge, C. T.; Schmitt, K. D.; Chu, C. T. W.; Olson, D. H.; Sheppard, E. W.; McCullen, S. B.; Higgins, J. B.; Schlenker, J. L. *J. Am. Chem. Soc.* **1992**, *114*, 10834−10843.

(2) Inagaki, S.; Fukushima, Y.; Kuroda, K. *J. Chem. Soc., Chem. Commun.* **1993**, 680−682.

(3) Wan, Y.; Shi, Y.; Zhao, D. *Chem. Commun.* **2007**, 897−926.

(4) Ying, J. Y.; Mehnert, C. P.; Wong, M. S. *Angew. Chem., Int. Ed.* **1999**, *38*, 56−77.

(5) Zhao, D.; Huo, Q.; Feng, J.; Chmelka, B. F.; Stucky, G. D. *J. Am. Chem. Soc.* **1998**, *120*, 6024−6036.

(6) Monnier, A.; Schueth, F.; Huo, Q.; Kumar, D.; Margolese, D.; Maxwell, R. S.; Stucky, G. D.; Krishnamurty, M.; Petroff, P.; Firouzi, A.; Janicke, M.; Chmelka, B. F. *Science* **1993**, *261*, 1299−1303.

(7) Tian, Z.-R.; Tong, W.; Wang, J.-Y.; Duan, N.-G.; Krishnan, V. V.; Suib, S. L. *Science* **1997**, *276*, 926−930.

(8) Huo, Q.; Margolese, D. I.; Ciesla, U.; Feng, P.; Gier, T. E.; Sieger, P.; Leon, R.; Petroff, P. M.; Schueth, F.; Stucky, G. D. *Nature* **1994**, *368*, 317−321.

(9) Yang, P.; Zhao, D.; Margolese, D. I.; Chmelka, B. F.; Stucky, G. D. *Nature* **1998**, *396*, 152−155.

(10) Braun, P. V.; Osenar, P.; Stupp, S. I. *Nature* **1996**, *380*, 325−328.

(11) Antonelli, D. M.; Ying, J. Y. *Angew. Chem., Int. Ed.* **1996**, *35*, 426−430.

(12) Huo, Q.; Liu, J.; Wang, L.-Q.; Jiang, Y.; Lambert, T. N.; Fang, E. *J. Am. Chem. Soc.* **2006**, *128*, 6447−6453.

(13) Liu, J.; Yang, Q.; Zhang, L.; Yang, H.; Gao, J.; Li, C. *Chem. Mater.* **2008**, *20*, 4268−4275.

(14) Liu, X.; Li, X.; Guan, Z.; Liu, J.; Zhao, J.; Yang, Y.; Yang, Q. *Chem. Commun.* **2011**, *47*, 8073−8075.
(15) Yuan, J.-J.; Mykhaylyk, O. O.; Ryan, A. J.; Armes, S. P. *J. Am. Chem. Soc.* **2007**, *129*, 1717−1723.
(16) Khanal, A.; Inoue, Y.; Yada, M.; Nakashima, K. *J. Am. Chem. Soc.* **2007**, *129*, 1534−1535.
(17) Yu, K.; Hurd, A. J.; Eisenberg, A.; Brinker, C. J. *Langmuir* **2001**, *17*, 7961−7965.
(18) Smarsly, B.; Xomeritakis, G.; Yu, K.; Liu, N.; Fan, H.; Assink, R. A.; Drewien, C. A.; Ruland, W.; Brinker, C. J. *Langmuir* **2003**, *19*, 7295−7301.
(19) Yu, K.; Smarsly, B.; Brinker, C. J. *Adv. Funct. Mater.* **2003**, *13*, 47−52.
(20) Yu, K.; Wu, X.; Brinker, C. J.; Ripmeester, J. *Langmuir* **2003**, *19*, 7282−7288.
(21) Kruk, M.; Hui, C. M. *J. Am. Chem. Soc.* **2008**, *130*, 1528−1529.
(22) Huang, L.; Yan, X.; Kruk, M. *Langmuir* **2010**, *26*, 14871−14878.
(23) Mandal, M.; Kruk, M. *J. Phys. Chem. C* **2010**, *114*, 20091−20099.
(24) Kruk, M.; Hui, C. M. In *Hybrid Nanomaterials: Synthesis, Characterization, and Applications*; Chauhan, B. P. S., Ed.; Wiley: 2011; pp 285−297.
(25) Deng, Y.; Yu, T.; Wan, Y.; Shi, S.; Meng, Y.; Gu, D.; Zhang, L.; Huang, Y.; Liu, C.; Wu, X.; Zhao, D. *J. Am. Chem. Soc.* **2007**, *129*, 1690−1697.
(26) Mal, N. K.; Fujiwara, M.; Tanaka, Y. *Nature* **2003**, *421*, 350−353.
(27) Van Der Voort, P.; Ravikovitch, P. I.; De Jong, K. P.; Benjelloun, M.; Van Bavel, E.; Janssen, A. H.; Neimark, A. V.; Weckhuysen, B. M.; Vansant, E. F. *J. Phys. Chem. B* **2002**, *106*, 5873−5877.
(28) Kruk, M.; Jaroniec, M.; Joo, S. H.; Ryoo, R. *J. Phys. Chem. B* **2003**, *107*, 2205−2213.
(29) Celer, E. B.; Kruk, M.; Zuzek, Y.; Jaroniec, M. *J. Mater. Chem.* **2006**, *16*, 2824−2833.
(30) Cao, L.; Man, T.; Kruk, M. *Chem. Mater.* **2009**, *21*, 1144−1153.
(31) Kruk, M.; Cao, L. *Langmuir* **2007**, *23*, 7247−7254.
(32) Mandal, M.; Kruk, M. *J. Mater. Chem.* **2010**, *20*, 7506−7516.
(33) Kruk, M.; Jaroniec, M.; Ko, C. H.; Ryoo, R. *Chem. Mater.* **2000**, *12*, 1961−1968.
(34) Kruk, M.; Jaroniec, M.; Sayari, A. *Langmuir* **1997**, *13*, 6267−6273.
(35) Kruk, M.; Jaroniec, M. *Chem. Mater.* **2003**, *15*, 2942−2949.
(36) Huang, L.; Kruk, M. *J. Colloid Interface Sci.* **2012**, *365*, 137−142.
(37) Zhao, D.; Feng, J.; Huo, Q.; Melosh, N.; Frederickson, G. H.; Chmelka, B. F.; Stucky, G. D. *Science* **1998**, *279*, 548−552.
(38) Ryoo, R.; Ko, C. H.; Kruk, M.; Antochshuk, V.; Jaroniec, M. *J. Phys. Chem. B* **2000**, *104*, 11465−11471.
(39) Matos, J. R.; Mercuri, L. P.; Kruk, M.; Jaroniec, M. *Chem. Mater.* **2001**, *13*, 1726−1731.
(40) Shin, H. J.; Ryoo, R.; Kruk, M.; Jaroniec, M. *Chem. Commun.* **2001**, 349−350.
(41) Zhang, F.; Yan, Y.; Yang, H.; Meng, Y.; Yu, C.; Tu, B.; Zhao, D. *J. Phys. Chem. B* **2005**, *109*, 8723−8732.
(42) Cao, L.; Kruk, M. *J. Colloid Interface Sci.* **2011**, *361*, 472−476.
(43) Inagaki, S.; Guan, S.; Fukushima, Y.; Ohsuna, T.; Terasaki, O. *J. Am. Chem. Soc.* **1999**, *121*, 9611−9614.
(44) Melde, B. J.; Holland, B. T.; Blanford, C. F.; Stein, A. *Chem. Mater.* **1999**, *11*, 3302−3308.
(45) Asefa, T.; MacLachlan, M. J.; Coombs, N.; Ozin, G. A. *Nature* **1999**, *402*, 867−871.
(46) Kuroki, M.; Asefa, T.; Whitnal, W.; Kruk, M.; Yoshina-Ishii, C.; Jaroniec, M.; Ozin, G. A. *J. Am. Chem. Soc.* **2002**, *124*, 13886−13895.
(47) Fan, J.; Yu, C.; Wang, L.; Tu, B.; Zhao, D.; Sakamoto, Y.; Terasaki, O. *J. Am. Chem. Soc.* **2001**, *123*, 12113−12114.
(48) Yuan, P.; Tan, L.; Pan, D.; Guo, Y.; Zhou, L.; Yang, J.; Zou, J.; Yu, C. *New J. Chem.* **2011**, *35*, 2456−2461.
(49) Ruthstein, S.; Schmidt, J.; Kesselman, E.; Talmon, Y.; Goldfarb, D. *J. Am. Chem. Soc.* **2006**, *128*, 3366−3374.
(50) Sundblom, A.; Oliveira, C. L. P.; Pedersen, J. S.; Palmqvist, A. E. C. *J. Phys. Chem. C* **2010**, *114*, 3483−3492.
(51) Flodstrom, K.; Teixeira, C. V.; Amenitsch, H.; Alfredsson, V.; Linden, M. *Langmuir* **2004**, *20*, 4885−4891.
(52) Zhao, D. Y.; Yang, P. D.; Melosh, N.; Feng, Y. L.; Chmelka, B. F.; Stucky, G. *Adv. Mater.* **1998**, *10*, 1380−1385.
(53) Feng, P.; Bu, X.; Stucky, G. D.; Pine, D. J. *J. Am. Chem. Soc.* **2000**, *122*, 994−995.
(54) Volksen, W.; Miller, R. D.; Dubois, G. *Chem. Rev.* **2010**, *110*, 56−110.
(55) Lee, B.; Park, Y.-H.; Hwang, Y.-T.; Oh, W.; Yoon, J.; Ree, M. *Nat. Mater.* **2005**, *4*, 147−150.